

Dielectric and piezoelectric properties of hydroxyapatite-BaTiO₃ composites

C. R. Bowen,^{a)} J. Gittings, and I. G. Turner

Materials Research Centre, Department of Mechanical Engineering, University of Bath, Bath BA2 7AY, United Kingdom

F. Baxter and J. B. Chaudhuri

Centre for Regenerative Medicine, Department of Chemical Engineering, University of Bath, Bath BA2 7AY, United Kingdom

(Received 27 April 2006; accepted 30 July 2006; published online 28 September 2006)

This letter describes the relationships between the composition and the dielectric and piezoelectric properties of hydroxyapatite-barium titanate composites for polarized bone substitutes. The ac conductivity and permittivity were characterized from 0.1 Hz to 1 MHz, along with measurements of the d_{33} piezoelectric charge coefficient. The addition of BaTiO₃ led to an increase in permittivity and ac conductivity of the material. The increase in both properties was attributed to the presence of the high permittivity ferroelectric phase. The d_{33} and g_{33} coefficients decreased rapidly as hydroxyapatite was introduced into BaTiO₃ material. Composites below 80% by volume of BaTiO₃ exhibited no net piezoelectric effect. © 2006 American Institute of Physics.

[DOI: 10.1063/1.2355458]

A wide variety of calcium phosphate based bone replacement materials has been developed in recent years, mainly in the form of hydroxyapatite (HA). They have been used as bone fillers or coatings in orthopedic, dental, and maxillofacial applications and as tissue engineering scaffolds.¹ Recent research has found enhanced bone osteobonding and new bone growth on polarized hydroxyapatite due to the generation of a permanent surface charge.²⁻⁵ The surface charge is not due to dipole rotation, as in ferroelectric materials, but is thought to develop from proton migration in the columnar OH⁻ structure of hydroxyapatite under an applied electric field at elevated temperatures.³ It has been shown that bone growth is accelerated on the negatively charged surface of polarized hydroxyapatite and decelerated on the positive surface.^{2,4} The mechanism is not clear, but rapid bone formation on negative surfaces is possibly due to adsorption of Ca²⁺ ions, which act as nuclei for calcium phosphate formation.

In addition to HA polarization, it is known that bone is piezoelectric⁶ and develops a charge under the application of a mechanical stress. It has been hypothesized that stress induced potentials in bone influence the activity of osseous (bone) cells.⁷ As a result, piezoelectric materials have attracted interest in medical applications, for example, using piezoelectric polyvinylidene fluoride polymer film.^{8,9} Park *et al.*¹⁰ and Hwang *et al.*¹¹ considered crystal growth formation on piezoelectric BaTiO₃ *in vitro*. Calcium phosphate crystals rapidly grew on the negatively charged surface, but not on the positive surface, indicating that polarized BaTiO₃ can improve bioactivity. The dielectric properties of HA have also been studied since electromagnetic fields accelerate bone healing.¹²

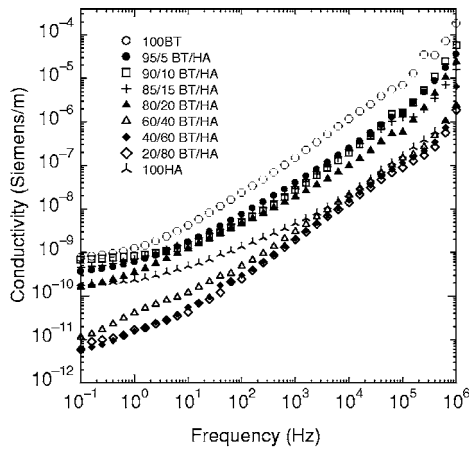
Limited research has attempted to combine the bioactive properties of HA with a piezoelectric and high permittivity ferroelectric material, such as BaTiO₃. Feng *et al.*¹³ prepared HA-BaTiO₃ composites, which promoted osteogenesis in

the jawbones of dogs. No reaction phases between the two phases were observed from x-ray diffraction (XRD) analysis and the composites exhibited a d_{33} piezoelectric charge coefficient of 6 pC/N. There was, however, no indication of the precise composition of the composites. Almeida *et al.*¹⁴ presented optical and electrical properties of screen-printed HA-BaTiO₃ thick films along with a detailed XRD study, but no piezoelectric properties. In the present work we study HA-BaTiO₃ composites to understand the relationship between the composition and the dielectric and piezoelectric properties of the materials.

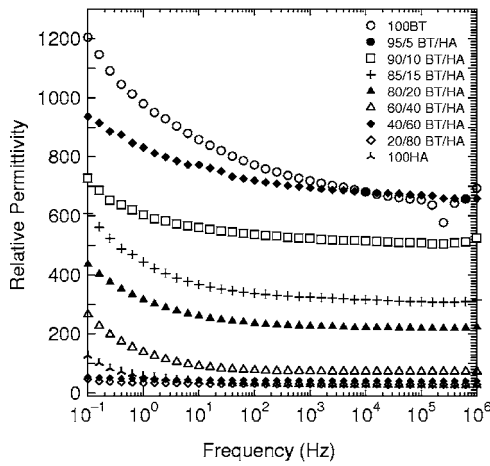
HA-BaTiO₃ composites were manufactured via pressureless sintering with BaTiO₃ contents varying from 0% to 100% by volume. After ball milling in zirconia media with a polyethylene glycol binder, powder compacts were cold pressed at 100 MPa. The diameter of the compacts was 15 mm with a thickness of ~2 mm. The composites were sintered in air at 1300 °C for 2 h with a heating and cooling ramp rate of 60 °C/h. After sintering the materials were ground flat and conducting silver ink electrodes were applied (RS Products 101-5621). Materials were corona poled, whereby a high potential difference was applied across the sample by a high-tension point source.¹⁵ Poling was carried out at 130 °C using a potential of 28 kV and a point source height of 70 mm. The process does not require an oil bath for heating, which could contaminate the material for biocompatibility testing. The d_{33} coefficient was measured using a Take Control PM25 piezometer. Permittivity and ac conductivity were measured from 0.1 Hz to 1 MHz at room temperature using a Solatron 1260 impedance analyzer and a 1296 dielectric interface using a voltage of 1 V_{rms}.

Figure 1(a) shows the variation in real part of ac conductivity (σ) as a function of frequency for all the composite compositions. At low frequencies (<10 Hz) there is a little or no frequency dependence for many of the composites. For higher frequencies (>100 Hz) the ac conductivity rises almost linearly with frequency (f), following “universal” power law behavior¹⁶ such that

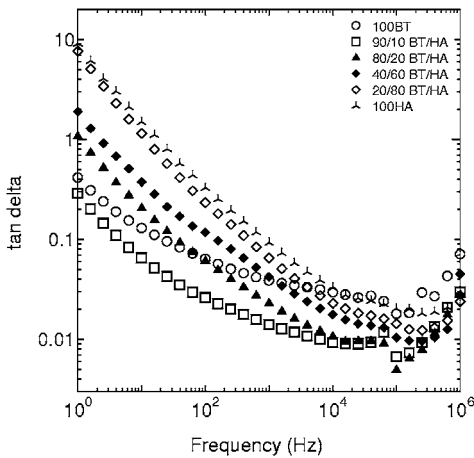
^{a)}Electronic mail: c.r.bowen@bath.ac.uk



(a)



(b)



(c)

FIG. 1. (a) Real part of ac conductivity (σ) for HA–BaTiO₃ composites. The legend indicates the volume fraction of BaTiO₃ (BT) and hydroxyapatite (HA). (b) Relative permittivity (ϵ) for HA–BaTiO₃ composites. The legend indicates the volume fraction of BaTiO₃ (BT) and hydroxyapatite (HA). (c) Loss tangent for selected HA–BaTiO₃ composites. The legend indicates the volume fraction of BaTiO₃ (BT) and hydroxyapatite (HA).

$$\sigma(\omega)\alpha\omega^n, \tag{1}$$

where ω is angular frequency ($2\pi f$) and, from Fig. 1(a), n is $0.80 < n < 0.97$. Examination of Fig. 1(a) reveals that, for all the composites studied, the ac conductivity at a particular frequency increases with increasing BaTiO₃ content. Shi *et al.*¹⁷ recently manufactured a range of HA–Ti₃SiC₂ compos-

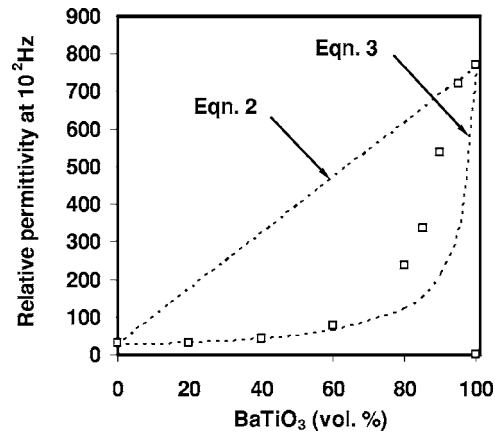


FIG. 2. Relative permittivity at 10^2 Hz for HA–BaTiO₃ composites. The lines represent Wiener bounds [Eqs. (2) and (3)].

ites and characterized their electrical properties in a similar frequency range.¹⁸ The increase in conductivity for HA–Ti₃SiC₂ composites was due to an increasing volume fraction of conducting Ti₃SiC₂. However, HA–BaTiO₃ composites consist of two relatively insulating phases, as seen from the low frequency conductivities of pure BaTiO₃ and HA in Fig. 1(a). Using microstructural electrical networks¹⁹ it has been shown that the ac conductivity (admittance) of the insulating phases, $\omega\epsilon\epsilon_0$, can contribute to the conductivity in the power law region, where ϵ is the relative permittivity of the phase (HA or BaTiO₃) and ϵ_0 is the permittivity of free space. Since the permittivity of BaTiO₃ is much greater than HA (see Figs. 2 and 3), the higher $\omega\epsilon\epsilon_0$ of BaTiO₃ leads to an increase in ac conductivity with increasing BaTiO₃ content.

The frequency dependence of the relative permittivity is shown in Fig. 1(b), which indicates that all the samples show a degree of dielectric dispersion (<10 Hz). The permittivity magnitude and degree of dispersion decrease with decreasing BaTiO₃ content, although pure HA also exhibits a dispersion. The HA dispersion has been attributed by Mahabole *et al.*²⁰ to the dipole moment of hydroxyl ions in HA, although the presence of a dc conductivity in the material can lead to a similar response.^{19,21} Figure 1(c) shows the loss tangent for selected composites. After an initial decrease, the loss increases with increasing HA content. To indicate the variation of permittivity with composite composition, Fig. 2 shows the relative permittivity at 10^2 Hz as a function of BaTiO₃ content. The composite permittivity values are within the series and parallel Wiener bounds,²² Eqs. (2) and (3),

$$\epsilon_{\text{composite}} = v_{\text{HA}}\epsilon_{\text{HA}} + v_{\text{BaTiO}_3}\epsilon_{\text{BaTiO}_3}, \tag{2}$$

$$\frac{1}{\epsilon_{\text{composite}}} = \frac{v_{\text{HA}}}{\epsilon_{\text{HA}}} + \frac{v_{\text{BaTiO}_3}}{\epsilon_{\text{BaTiO}_3}}, \tag{3}$$

where ϵ_x is the permittivity of material x and v_x is the volume fraction.

The piezoelectric d_{33} coefficient for the composites is shown in Fig. 3. The addition of HA to BaTiO₃ leads to a rapid decrease in d_{33} . Composites below 80% by volume of BaTiO₃ exhibited no piezoelectric effect ($d_{33}=0$ pC/N). In piezoelectric-polymer composites the polymer can mechanically clamp the piezoelectric and prevent it from developing

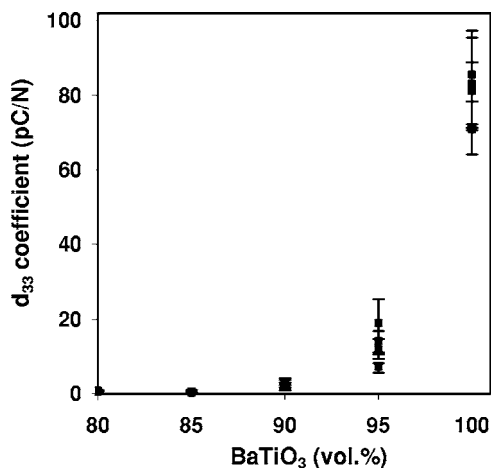


FIG. 3. Piezoelectric charge coefficient (d_{33}) at 97 Hz for HA–BaTiO₃ composites. The error bars are the maximum and minimum values.

a strain during the poling process. This can lead to mechanical depolarization and loss of piezoelectric properties.²³ For HA–BaTiO₃ composites the hydroxyapatite ceramic is much stiffer than a polymer and the increased level of matrix “clamping” could account for the rapid decrease in d_{33} . Figure 3 reveals that HA–BaTiO₃ composites must have a high BaTiO₃ content (>90 vol %) to achieve the d_{33} of 6 pC/N reported by Feng *et al.*¹³

The permittivity and d_{33} are used to estimate the stress induced potential by calculation of the piezoelectric voltage coefficient, g_{33} ($=d_{33}/\epsilon_{\text{composite}}$), the electric field produced per unit stress. Since the d_{33} decreases more rapidly than the permittivity, the g_{33} coefficient decreases from approximately $18 \times 10^{-3} \text{ V m}^{-1} \text{ Pa}^{-1}$ for 100% BaTiO₃ to 3.5×10^{-3} and $2.1 \times 10^{-3} \text{ V m}^{-1} \text{ Pa}^{-1}$ for composites containing 95 and 90 vol % BaTiO₃, respectively. Considering a modest stress of 1 MPa applied to a 10% HA–90% BaTiO₃ composite of thickness of 100 μm , a potential of 0.2 V is generated, a value similar to that reported by Marino *et al.*⁹ on piezoelectric polyvinylidene fluoride²² which was shown to enhance bone formation. In summary, this letter presents an

understanding of the composition-dielectric-piezoelectric property relationships for HA–BaTiO₃ composites as polarized bone substitutes.

The authors would like to thank the U.K. Engineering and Physical Sciences Research Council for funding.

¹M. Vallet-Regi and J. M. Gonzalez-Calbert, *Prog. Solid State Chem.* **32**, 1 (2004).

²R. Kato, S. Nakamura, K. Katayama, and K. Yamashita, *J. Biomed. Mater. Res.* **74A**, 652 (2005).

³S. Nakamura, H. Takeda, and U. Kimihiro, *J. Appl. Phys.* **89**, 5386 (2001).

⁴T. Kobayashi, S. Nakamura, and K. Yamashita, *J. Biomed. Mater. Res.* **57**, 477 (2001).

⁵S. Nakamura, T. Kobayashi, and K. Yamashita, *J. Biomed. Mater. Res.* **61**, 593 (2002).

⁶E. Fukada and I. J. Yasuda, *J. Phys. Soc. Jpn.* **12**, 1158 (1957).

⁷C. A. L. Bassett and R. O. Becker, *Science* **137**, 1063 (1962).

⁸N. Moriyama and T. Ohnishi, U.S. Patent No. 5,684,061 (4 November 1997).

⁹A. A. Marino, J. Rosson, E. Gonzalez, L. Jones, S. Rogers, and E. Fukada, *J. Electrostat.* **21**, 347 (1988).

¹⁰Y. J. Park, K. S. Hwang, J. E. Song, J. L. Ong, and H. R. Rawls, *Biomaterials* **23**, 3859 (2002).

¹¹K. S. Hwang, J. E. Song, J. W. Jo, H. S. Yang, Y. J. Park, J. L. Ong, and H. R. Rawls, *J. Mater. Sci. Lett.* **13**, 133 (2002).

¹²T. P. Hoepfner and E. D. Case, *J. Biomed. Mater. Res.* **60**, 643 (2002).

¹³J. Q. Feng, H. P. Yuan, and X. D. Zhang, *Biomaterials* **18**, 1531 (1997).

¹⁴A. F. L. Almeida, P. B. A. Fechine, J. M. Sasaki, A. P. Ayala, J. C. Goes, D. L. Pontes, W. Margulis, and A. S. B. Sombra, *Solid State Sci.* **6**, 267 (2004).

¹⁵D. Waller and A. Safari, *Ferroelectrics* **87**, 189 (1988).

¹⁶A. K. Jonscher, *Nature (London)* **253**, 717 (1975).

¹⁷S. L. Shi, W. Pan, M. H. Fang, and Z. Y. Fang, *J. Am. Ceram. Soc.* **89**, 743 (2006).

¹⁸S. L. Shi, W. Pan, R. B. Han, and C. L. Wan, *Appl. Phys. Lett.* **88**, 052903 (2006).

¹⁹D. P. Almond and C. R. Bowen, *Phys. Rev. Lett.* **92**, 157601 (2004).

²⁰M. P. Mahabole, R. C. Aiyer, C. V. Ramakrishna, B. Sreedhar, and R. S. Khairnar, *Bull. Mater. Sci.* **28**, 535 (2005).

²¹A. V. Turik, G. S. Radchenko, A. I. Chernobabov, and S. A. Turik, *JETP Lett.* **79**, 407 (2004).

²²K. K. Karkkainen, A. H. Sihvola, and K. I. Nikoskinen, *IEEE Trans. Geosci. Remote Sens.* **38**, 1303 (2000).

²³T. Hauke, R. Steinhausen, W. Seifert, H. Beige, and M. Kamlah, *J. Appl. Phys.* **89**, 5040 (2001).